VII International Conference on Computational Methods in Marine Engineering
MARINE 2017
M. Visonneau, P. Queutey and D. Le Touzé (Eds)

NUMERICAL SIMULATION OF AN ARRAY OF HEAVING FLOATING POINT ABSORBER WAVE ENERGY CONVERTERS USING OPENFOAM

BRECHT DEVOLDER[1,2], PIETER RAUWOENS[2] AND PETER TROCH[1]

[1] Ghent University
Department of Civil Engineering
Technologiepark 904, 9052 Ghent, Belgium
e-mail: Brecht.Devolder@UGent.be, Peter.Troch@UGent.be

[2] KU Leuven
Technology Campus Ostend, Department of Civil Engineering
Zeedijk 101, 8400 Ostend, Belgium
e-mail: pieter.rauwoens@kuleuven.be

Key words: Wave energy, floating point absorber, array, CFD modelling, experimental validation

Abstract. In this paper we use the CFD toolbox OpenFOAM to perform numerical simulations of multiple floating point absorber Wave Energy Converters (WECs) in a numerical wave basin. The two-phase Navier-Stokes fluid solver is coupled with a motion solver to simulate the wave-induced rigid body heave motion. The key of this paper is to extend numerical simulations of a single WEC unit to multiple WECs and to tackle the issues of modelling individual floating objects close to each other in an array lay-out. The developed numerical model is validated with laboratory experiments for free decay tests and for a regular wave train using two or five WECs in the array. For all the simulations presented, a good agreement is found between the numerical and experimental results for the WECs' heave motions, the surge forces on the WECs and the perturbed wave field. As a result, our coupled CFD–motion solver proofs to be a suitable and accurate toolbox for the study of wave-structure interaction problems of multiple floating bodies in an array configuration.

1 INTRODUCTION

Wave energy from ocean waves is captured by Wave Energy Converters (WECs) and converted into electrical power. In this study, WECs of the floating point absorber (FPA) type are selected. The numerically obtained viscous flow field around and the response of a single WEC unit have been validated with experimental data in previous work of the authors [1]. Now, this study focusses on the hydrodynamics around and the response of a small array of two and five WECs respectively. However, this is a starting point for wave farm modelling in which the interaction between a large number of closely spaced WECs will be analysed.

The Computational Fluid Dynamics (CFD) toolbox OpenFOAM [2] is used to study array effects in a numerical wave basin by solving the three dimensional flow field around and the

response of the WECs. Moreover, CFD is able to include viscous, turbulent and non-linear effects which may be absent in simplified radiation-diffraction models such as potential flow solvers based on boundary element methods.

The main focus of the paper is put on the numerical simulation of several free decay tests using different array layouts. One WEC unit is initially placed out of equilibrium and released, leading to a damped oscillatory motion until all the forces acting on that WEC are in equilibrium. Moreover, the motion of the WEC generates radiated waves with decreasing wave heights away from the WEC. Those radiated waves initiate the motion of and a surge force on the neighbouring WECs in the array. Simulations are performed in order to compare the radiated wave field, the motion of and the surge force on the heaving WECs with experimental data measured in a wave basin. The purpose of the simulations is to demonstrate the ability of the coupled CFD–motion solver to simulate wave propagation of the radiated wave field in an array.

The second part of the paper is dedicated to present CFD simulations of an array of two WEC units subjected to a specific regular wave train. Only the heave motion of the WECs is considered and together with the perturbed wave field validated against laboratory results.

The capability of OpenFOAM to study wave-body interactions is already reported by [3]. An excellent description and comparison of the different numerical models for wave energy devices is provided in [4]. They mentioned that good agreements have been obtained between CFD and experimental results, demonstrating the feasibility of CFD simulations for wave energy applications. As mentioned before, simulations of a single WEC unit have been reported in previous work of the authors [1] but also in [5,6]. Numerical simulations of WEC arrays using simplified radiation-diffraction models have been published in [7–9]. However, CFD simulations of a WEC array have only been reported by a few researchers, e.g. [10,11].

2 EXPERIMENTAL SETUP

In this study, experimental data is used from the WECwakes project [12] conducted in the shallow water wave basin of the Danish Hydraulics Institute (DHI; Hørsholm, Denmark). Up to 25 WEC units were installed in the basin, which has a length of 25 m and a width of 35 m. For all the tests, a constant water depth of 0.70 m was maintained in the basin.

The WEC's geometry is depicted in Figure 1. The WECs are characterised by a mass m of 20.545 kg, a total height h_{WEC} of 0.60 m, a diameter D of 0.315 m and a draft d_{WEC} of 0.315 m. At the top of the WEC, the power-take off (PTO) system is installed (Figure 1). The PTO force is applied to the buoy by mimicking a Coulomb damper using friction brakes (composed of two PTFE-blocks and four springs) between the float and the supporting axis.

The enormous experimental database is of large interest for the validation and extension of different numerical models. In this paper, our coupled CFD–motion solver is validated by using the available experimental dataset generated during the WECwakes project.

3 NUMERICAL FRAMEWORK

Numerical modelling is performed for the study of individual WEC units configured in an array layout. The two-phase flow solver with dynamic mesh handling, interDyMFoam, is available in OpenFOAM to perform simulations of moving bodies installed in a numerical wave basin.

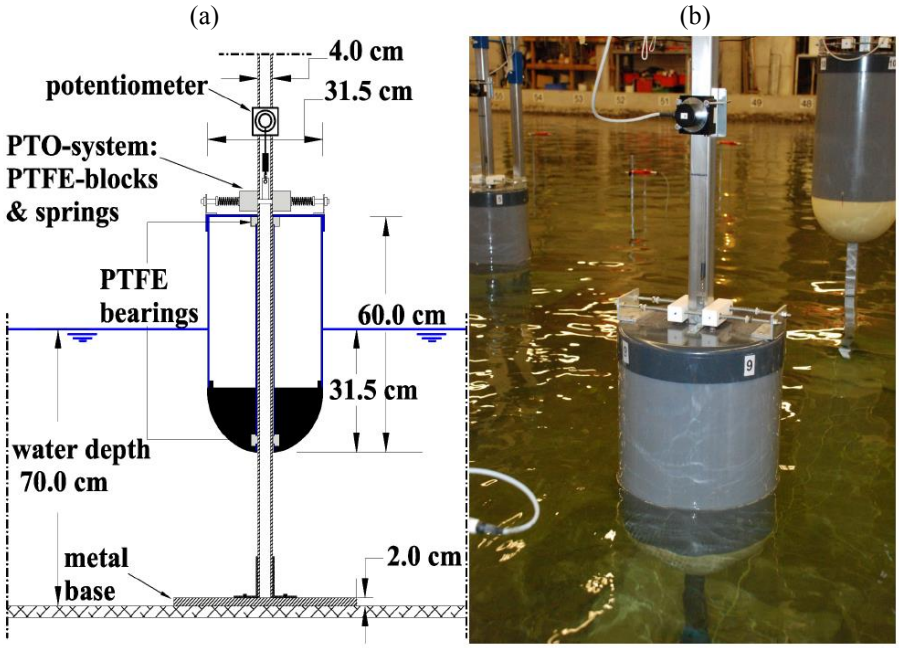

Figure 1: (a) Definition sketch of the cross section of a WEC unit; (b) photograph of a WEC unit within an array installed in the wave basin during the WECwakes project. Adopted from Stratigaki (2014).

3.1 Flow solver

Simulations of the two-phase flow field are performed by solving the incompressible RANS-equations, with a conservation equation for the Volume of Fluid (VoF) [13]. Turbulent effects are not dominating since the flow of the simulations presented is always characterised by a low Keulegan-Carpenter (KC) number. Therefore in the first instance, only laminar solutions are generated. However, in case turbulence plays a role, we refer to [14] on how to properly deal with turbulence near the air-water interface.

For all simulations the following settings are used: central discretisation for the pressure gradient and the diffusion terms; TVD (total variation diminishing) schemes with a van Leer limiter [15] for the divergence operators; second order, bounded, implicit time discretisation; a maximum Courant number of 0.30.

3.2 Computational domain

All the numerical simulations are performed in a numerical wave basin which represents the experimental wave basin as good as possible. However, some simplifications are made in order to obtain reasonable simulation times. Firstly, a vertical symmetry plane through the centre of the WECs is implemented over the length over the basin, as indicated in Figure 2 for the 5WEC-array. This is justified because the WECs tested in this paper are all installed in the middle of the basin and no asymmetric effects are expected (low KC numbers). For the free decay test using five WECs, a symmetrical heave motion of WEC2 and WEC4 and WEC1 and WEC5 is expected because the middle WEC (WEC3) is decaying and the spacing between the individual WECs is fixed to 5*D*. Therefore a second symmetry plane is implemented perpendicular to the first symmetry plane and through the centre of WEC3 (see Figure 2). Each boundary of the computational domain needs specific boundary conditions.

We use the IHFOAM toolbox [16,17] to implement the wavemaker and absorbing beach in the experimental facility. The side wall of the numerical wave basin is sufficiently far enough from the array, > 8*D*, to neglect its influence on the hydrodynamics around the WECs.

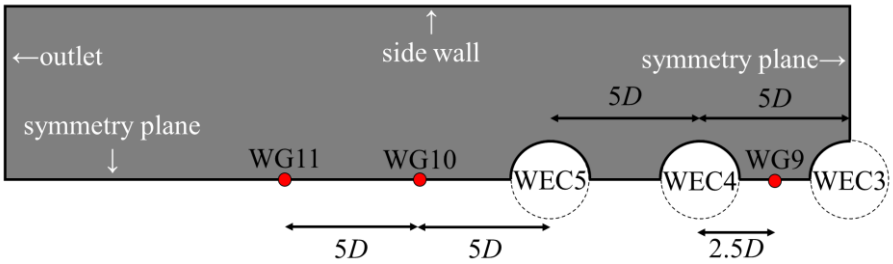

Figure 2: Plan view of the numerical wave basin for the 5WEC-array using two symmetry planes during a free decay test of WEC3. The red dots indicate the position of three wave gauges: WG9, WG10 and WG11.

The numerical wave basin is represented by a structured grid consisting of only hexahedral cells with local refinements in the zones of interest (i.e. around the free water surface and the WECs). A longitudinal cross section of the numerical domain around the WEC array during a free decay test is depicted in Figure 3 for the 5WEC-array. The vertical grid resolution is about 1 cm in the zones of interest, which is sufficiently according to [1]. The horizontal cell size increases towards the boundaries of the wave basin in order to limit the number of cells. The only exception is for the simulation where regular waves are generated at the inlet, in that case the horizontal cell size is kept constant towards the inlet boundary only. The high aspect ratio observed for the cells above the decaying WEC is explained in the next paragraph.

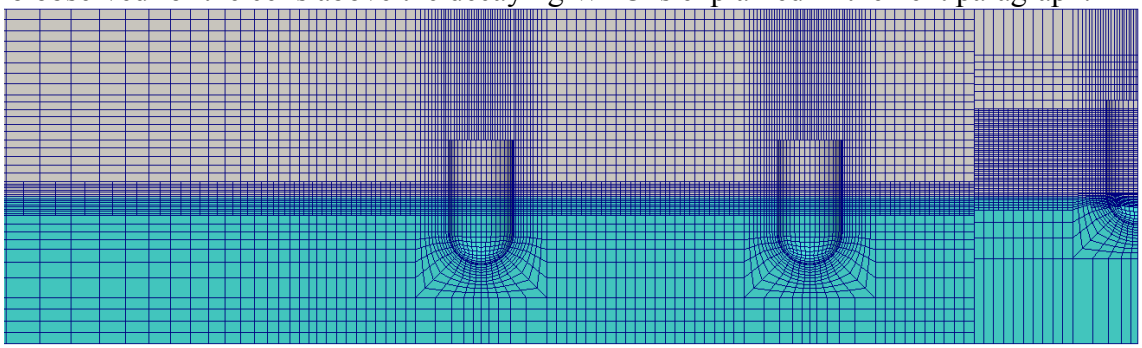

Figure 3: Cross section of the computational domain for the 5WEC-array (WEC3, WEC4 and WEC5), using two symmetry planes, during the initial condition of the free decay test of WEC3 (blue = water, grey = air).

3.3 Rigid body motion

The CFD-fluid solver is coupled with a motion solver in order to simulate rigid body motions. Only the governing motion of the WEC's behaviour is considered, the heave motion. During each time step in the transient simulation, an iterative procedure is needed to obtain a converged solution for both the fluid solver and the motion solver. We developed a method that accelerates this coupling procedure and hence reduces the amount of sub-iterations for each time step to four. The key ingredient of this method is a good estimator for the WEC's hydrodynamic added mass [18].

A second order accurate Crank-Nicolson integration scheme is used to derive the new position of the WEC from its acceleration *a*. The acceleration itself is based on Newton's

second law: $F = m \cdot a$ in which the force F is the sum of the pressure, shear and gravity forces acting on all the boundary faces of the WEC calculated with the fluid solver. The WEC's mass m is determined using the procedure developed in [1].

In order to simulate multiple independently moving WECs in an array configuration, arbitrary mesh interfaces (AMIs) are implemented in order to create sliding meshes (see dashed vertical lines in Figure 4 for the case of two WEC units). These AMIs define a zone of cells around each WEC unit. In each zone, only the lowest and highest row of cells (see blue shaded boxes in Figure 4) are expanded or compressed according to the motion of the WEC unit located in that zone. This is implemented to prevent undesirable mesh deformation around the air-water interface, enhancing the accuracy of the solution. As a consequence, high aspect ratios are obtained for the distorted cells at specific time instants. However, those cells are not inside the zones of interest and will therefore not affect the accuracy of the simulations. All the variables solved with the flow solver, such as velocity, pressure and volume fraction, are interpolated over the AMIs.

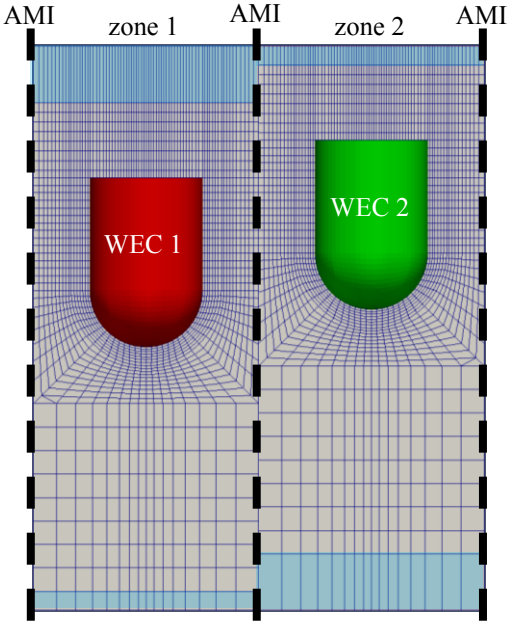

Figure 4: A definition sketch of two independently moving WECs inside a three-dimensional computational domain of hexahedral cells. Only the highest and lowest row of cells (blue shaded boxes) in a zone are distorted (expanded or compressed) according to the heave motion of the WEC located in that zone. In between the zones, AMIs are implemented to create sliding meshes (dashed lines).

4 RESULTS AND DISCUSSION

Numerical simulations of a small array are performed for two free decay tests and a regular wave train. Firstly, a free decay test is performed for both a 2WEC-array and a 5WEC-array by pushing one WEC down, release it instantaneously and monitor the response of the WEC itself, and the neighbouring WEC(s). Secondly, regular waves are generated to obtain the response of a 2WEC-array and the resulting perturbed wave field.

4.1 Free decay test using two WECs in a line, spacing = 5*D*

During this first test using a 2WEC-array, WEC5 is lifted higher than its equilibrium position, released, and a free decay test is started. At a distance of 5*D* = 1.575 m, WEC4 is freely floating in the water and will heave due to the radiated waves generated by WEC5.

In order to tune the numerical decaying motion to the experimental data, the methodology as reported in [1] is applied, resulting in a linear damper with a damping coefficient of 1.86 kg/s for WEC5. For WEC4, a much larger damping coefficient equal to 40 kg/s is used (see next section using the 5WEC-array). The resulting heave motions for WEC5 (decaying) and WEC4 (freely floating) are presented in Figure 5. It is clearly shown that the decaying motion of WEC5 is identical for the numerical and experimental model during the first 10 seconds. Thereafter, some small discrepancies are observed due to damping nonlinearities present during the experiments. It is however difficult to measure experimentally small heave motions due to friction of the bearings along the steel shaft (cfr. the WECwakes experiments). For WEC4, the resulting numerical heave motion is very small compared to the heave motion of WEC5. Unfortunately, the experimental recording failed for this test.

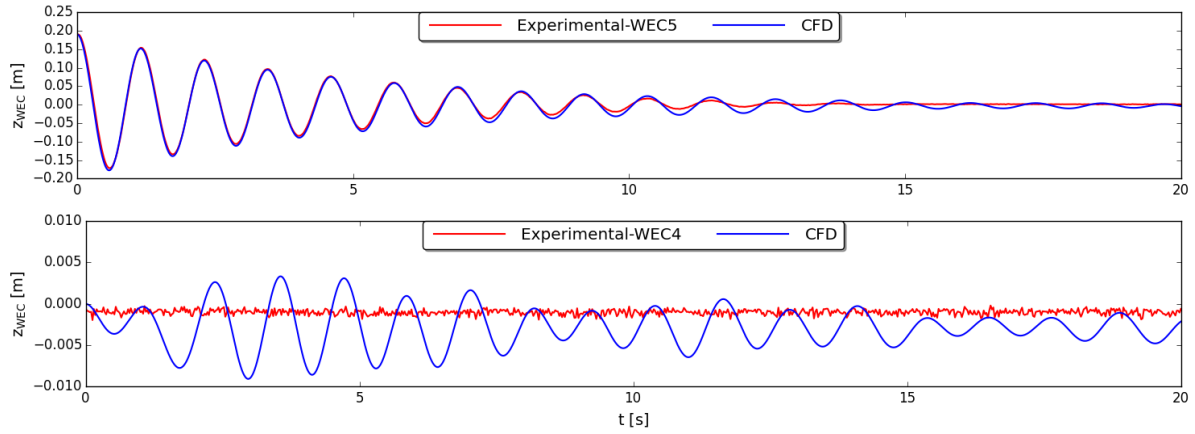

Figure 5: Vertical position of WEC5 (top) and WEC4 (bottom) during a free decay test of WEC5 with respect to its equilibrium position (z_{WEC} = 0 m) obtained with CFD (blue line) compared to experimental data (red line).

Additionally, the surge (horizontal) force on WEC4 due to the radiated wave field is compared between the numerical and experimental model and depicted in Figure 6. Again, a good comparison is found between both models. It is important to note that we filtered out the noise in the time signals of the experimental force measurements using a bandpass filter.

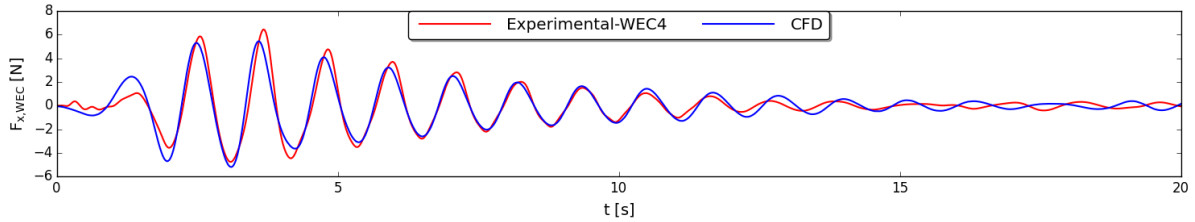

Figure 6: Surge force acting on WEC4 during a free decay test of WEC5 obtained with CFD (blue line) compared to the experimental determined surge force using two load cells after filtering the noise (red line).

Finally, the radiated wave field is given in Figure 7 for both numerical and experimental

data using the three wave gauges shown in Figure 2. The maximum observed amplitude of these radiated waves is smaller than 1 cm. Despite these small-amplitude waves, both results are very similar. In the first 10 seconds of the signals, the amplitude as well the phase of the radiated wave field is modelled close to the experimental results. Thereafter, some deviations between both results are observed due to the different behaviour of the numerical and experimental boundary conditions responsible for the absorption of the radiated waves.

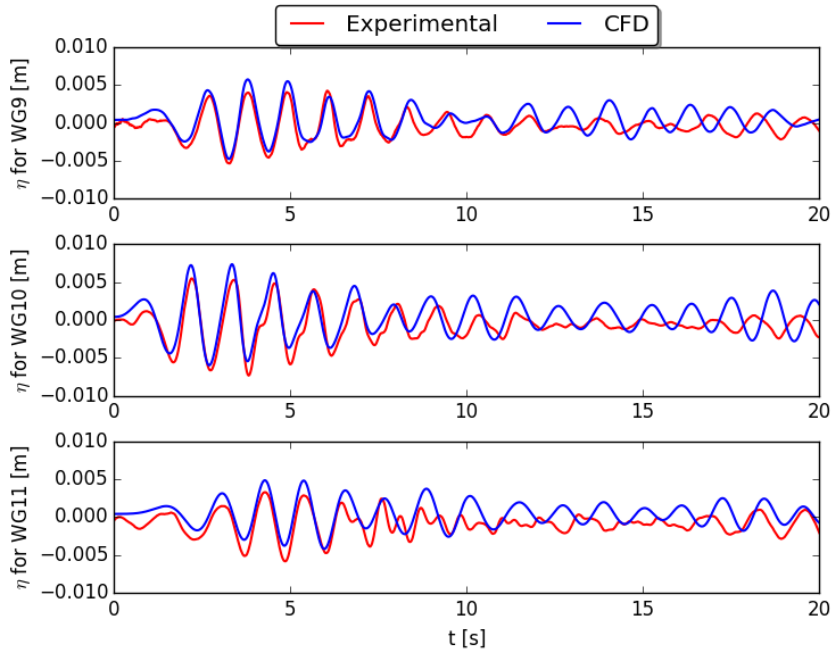

Figure 7: Radiated wave field around the 2WEC-array during a free decay test of WEC5 obtained with CFD (blue line) compared to the experimental measurements (red line).

4.2 Free decay test using five WECs in a line, spacing = 5*D*

The next test comprises a free decay test of a 5WEC-array in which WEC3 is lifted higher than its equilibrium position, released, and a free decay test is started. As presented before in Figure 2, the 5WEC-array is simplified to a 2.5WEC-array using two symmetry planes. WEC4 and WEC5, at a distance of 5*D* and 10*D* respectively, are freely floating in the water and will move due to the radiated waves generated by the decaying motion of WEC3.

The vertical position of WEC3 (decaying) and WEC4 and WEC5 (freely floating) are depicted in Figure 8 for both numerical and experimental data. As motivated in the previous paragraph, a linear damper is used for the three WECs simulated using a damping coefficient of 1.86 kg/s, 40 kg/s and 100 kg/s for WEC3, WEC4 and WEC5 respectively. The same conclusions are drawn for the decaying WEC3 as reported in the previous paragraph: a very good agreement is found between the numerical and experimental signal. Based on Figure 8, the values used for the linear damper of WEC4 and WEC5 are sufficiently accurate to obtain the same amplitudes in the time signal for both the numerical and experimental data. Interestingly, the damping coefficients for WEC4 and WEC5 are significantly larger than the one used for the decaying WEC3. As reported in [11], this is needed to take the influence of nonlinear stiction damping effects and bearing friction along the steel shaft into account for

small heave motions. It is also shown that the motion of WEC4 is closer to the experimental data compared to the motion of WEC5. This is due to the larger distance of WEC5 from the decaying WEC. Moreover, the experimental data reveal that the behaviour of WEC2 and WEC4 and WEC1 and WEC5 is not fully symmetrical. Additionally, the surge force on WEC4 and WEC5 due to the radiated wave field is compared between the numerical and experimental model and visualised in Figure 9. Again, a very good comparison is found between both models. Subsequently, the radiated wave field is given in Figure 10 for both numerical and experimental data using three wave gauges (see Figure 2). The maximum observed amplitude of these radiated waves is again smaller than 1 cm and a fair agreement is found between the numerical and experimental time series.

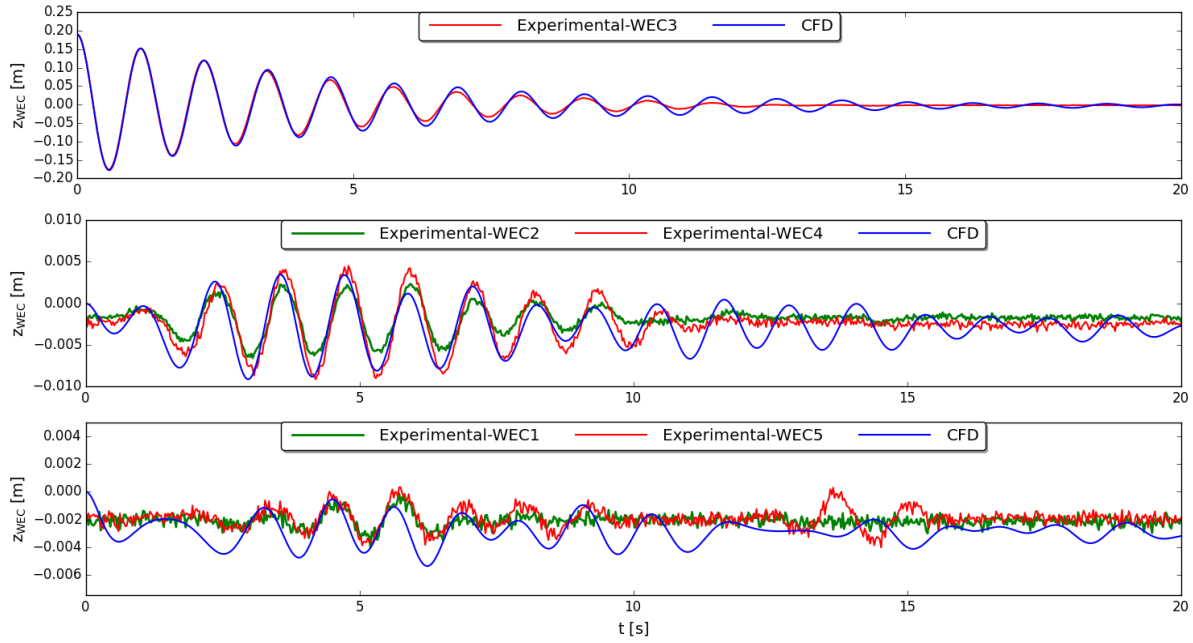

Figure 8: Vertical position of WEC3 (top), WEC4 (middle) and WEC5 (bottom) during a free decay test of WEC3 with respect to its equilibrium position ($z_{WEC} = 0$ m) obtained with CFD (blue line) compared to experimental data (green and red lines).

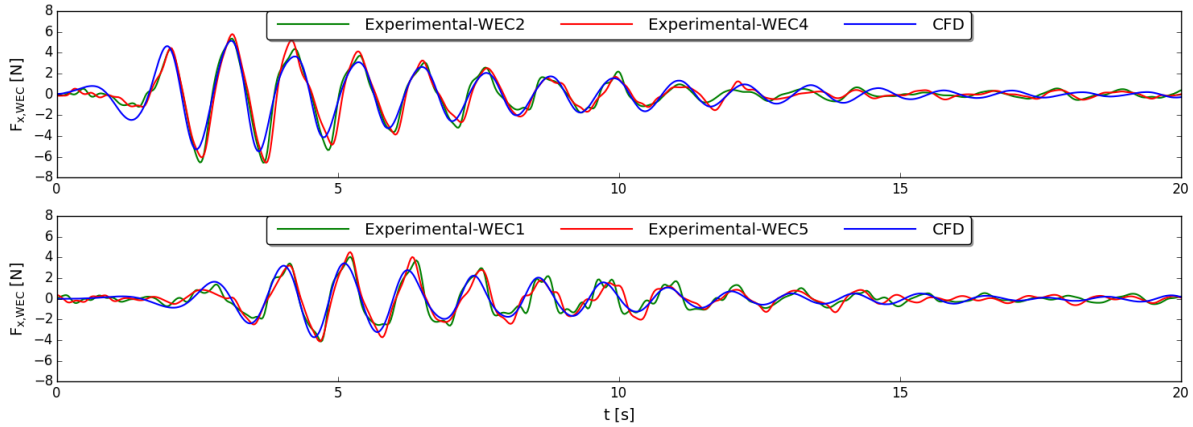

Figure 9: Surge force acting on WEC4 and WEC5 during a free decay test of WEC3 obtained with CFD (blue line) compared to the experimental determined surge forces after filtering the noise (green and red lines).

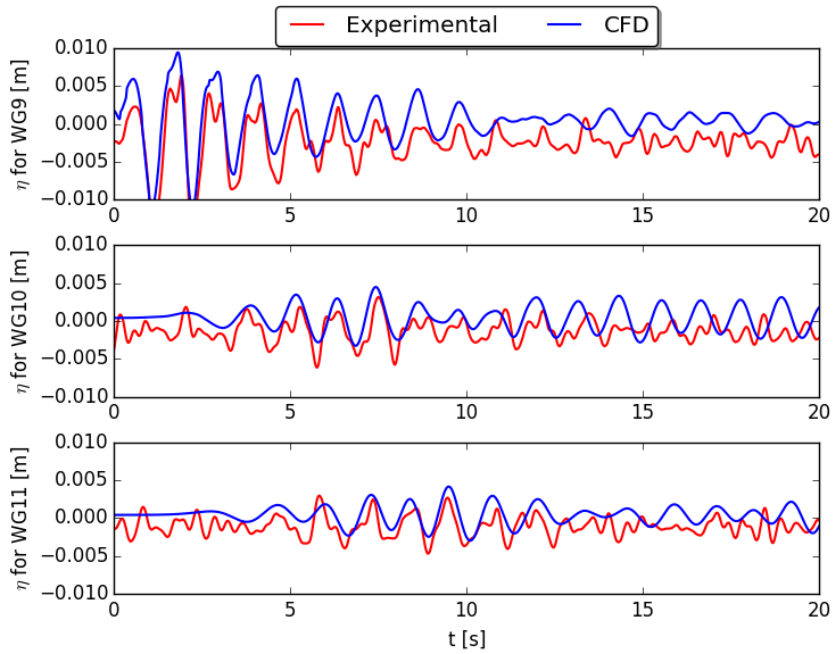

Figure 10: Radiated wave field around the 5WEC-array during a free decay test of WEC3 obtained with CFD (blue line) compared to the experimental measurements (red line).

4.3 Regular waves test using two WECs in a line, spacing = 5*D*

The last test presented in this paper includes the generation of regular waves and subject them to the 2WEC-array. The waves have a height H equal to 0.074 m, a wave period T of 1.26 s and are generated in a water depth d of 0.70 m. At the inlet, waves are generated using a second order Stokes theory and active wave absorption is turned on. For this simulation, a linear damper is used for both WECs with a damping coefficient of 1.86 kg/s. Moreover, a coulomb damper on each WEC is included because the PTO system was on during the experimental test. The PTO force is implemented in the numerical model as described in [12]:

$$F_{PTO} = -\mu F_{spring} sign(v(t)) = -\mu 4 dx k_{spring} sign(v(t)) \tag{2}$$

where $v(t)$ is the WEC's vertical velocity, $\mu = 0.17$, $dx = 30.5$ mm and $k_{spring} = 0.14$ N/mm.

The heave motions of both WECs are visualised in Figure 11 for the numerical and experimental model respectively. It is observed that the numerical obtained heave motions are significantly larger, about 60 %, than the experimental results. Moreover, there is a time shift present in the signals for both WECs. Figure 12 presents the surge force acting on both WECs when subjected to a regular wave train. In contrast as observed for the heave motions, the numerical obtained surge forces are very similar to the experimental data. Lastly, the perturbed wave field (i.e. incident + diffracted + radiated wave field) is given in Figure 13 for both numerical and experimental data using three wave gauges (see Figure 2). The time signals confirm that an identical wave field is present in the numerical wave basin as observed during the experimental tests.

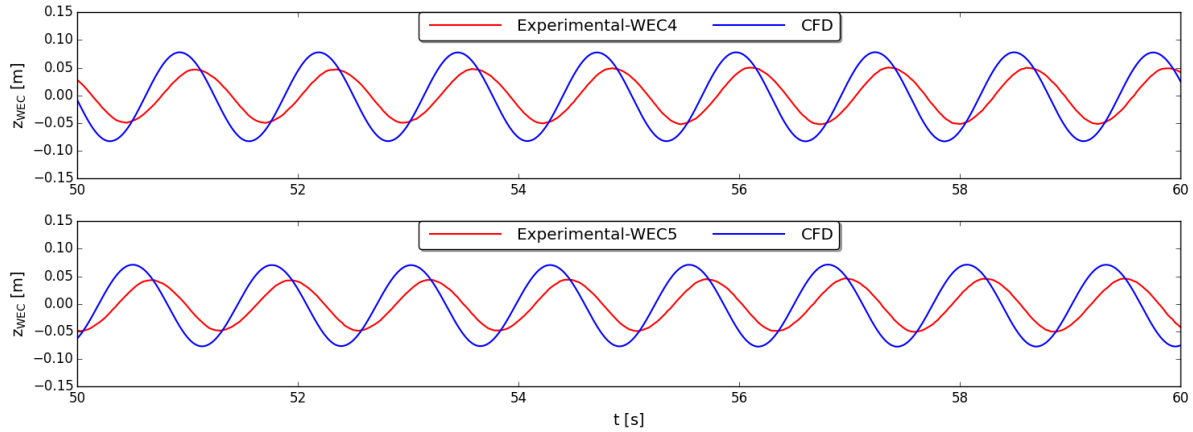

Figure 11: Vertical position of WEC4 (top) and WEC5 (bottom) during a regular wave test (H = 0.074 m, T = 1.26 s, d = 0.70 m) obtained with CFD (blue line) compared to the experimental heave motions (red line).

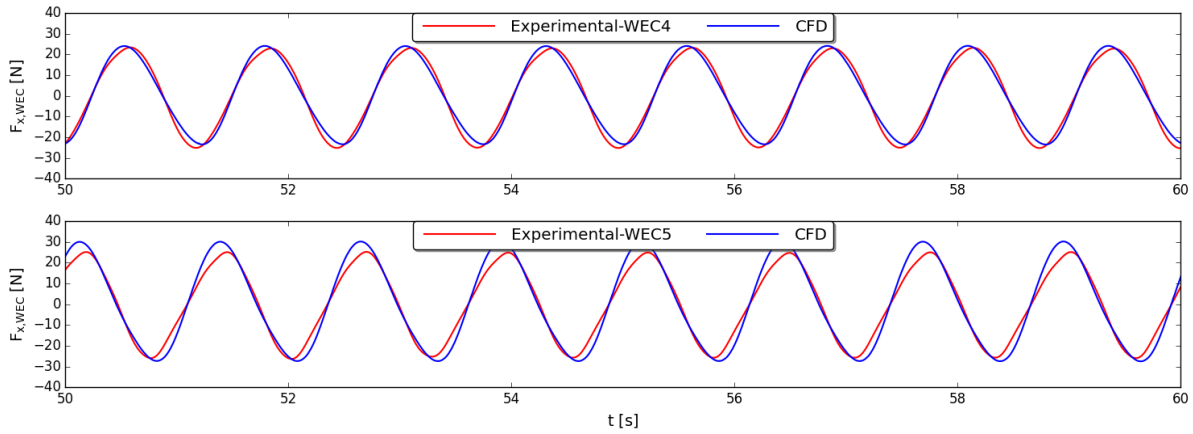

Figure 12: Surge force acting on WEC4 (top) and WEC5 (bottom) during a regular wave test (H = 0.074 m, T = 1.26 s, d = 0.70 m) obtained with CFD (blue line) compared to the experimental measurements after filtering the noise (red line).

As a conclusion, only a different behaviour in the WECs' heave motions (amplitude + time shift) is observed between numerical and experimental data. Therefore, we assume that those discrepancies are mainly related to the different behaviour of the PTO system between the numerical and experimental model, which needs further investigation.

5 RESEARCH TOPICS UNDER INVESTIGATION

The topics listed below will be investigated in the near feature:

- The sensitivity of the linear damper acting on each WEC unit;
- The PTO force needs to be implemented precisely in the numerical model for an accurate representation of the spring system's behaviour used during the experiments;
- Regular waves cause a net horizontal force acting on the WEC units inducing an additional vertical damping force (coulomb damper) apart from the PTO force applied;
- Including turbulent effects;
- Simulations of different numbers of WECs arranged in various layouts.

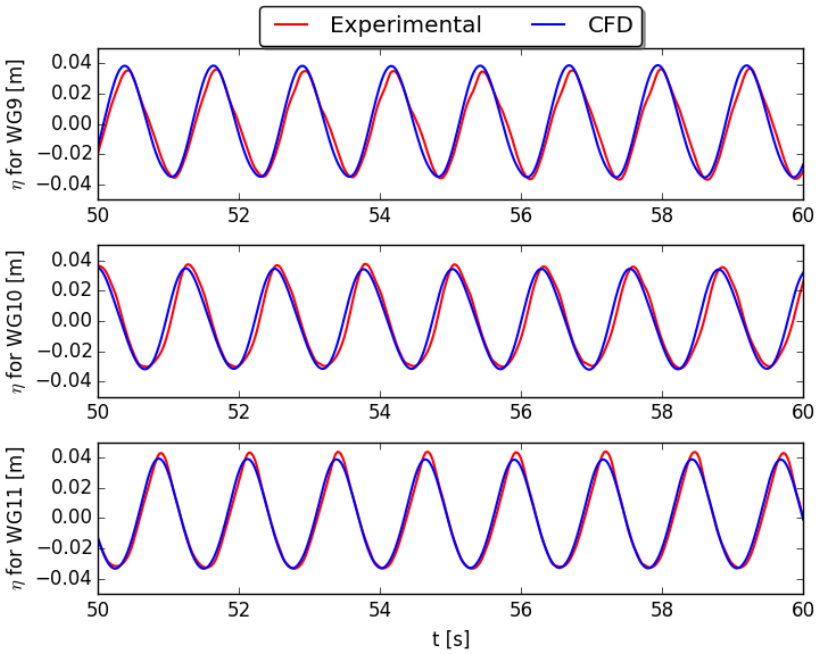

Figure 13: Perturbed wave field around the 2WEC-array during a regular wave test (H = 0.074 m, T = 1.26 s, d = 0.70 m) obtained with CFD (blue line) compared to the experimental data (red line).

6 CONCLUSIONS

We have presented several cases of numerical simulations of two and five heaving WECs installed in an array lay-out in a numerical wave basin. Regarding the free decay tests, a very good agreement is obtained between numerical and experimental results for both a 2WEC-array and a 5WEC-array. Not only the vertical position of the WECs and the surface elevations of the radiated wave field have shown an excellent agreement but also the surge force acting on the neighbouring WECs. Furthermore, simulations of an array of two WECs subjected to a specific regular wave train have returned promising results for its heave motion, the surge force on the WECs and the perturbed wave field around the WECs.

The numerical results have shown that our coupled CFD–motion solver is a robust and suitable toolbox to study wave-structure interaction. Moreover, the coupled model is accurate to analyse the interaction between multiple WECs installed in an array configuration. In particular, the surge force on the WECs and the perturbed wave field have been modelled very well. Future improvements will include a more accurate modelling of the PTO system to enhance the prediction of the WECs' heave motion.

7 ACKNOWLEDGEMENTS

The first author is Ph.D. fellow of the Research Foundation – Flanders (FWO), Belgium (Ph.D. fellowship 1133817N).

The WECwakes project is funded by the EU FP7 HYDRALAB IV programme (contract no. 261520). The project is a consortium of seven European partners coordinated by Ghent University-Belgium (Peter Troch; Vasiliki Stratigaki). The construction of the WEC models at Ghent University (research grant FWO-KAN-15 23 712 N) and part of the data pre- and

post-processing (Ph.D. funding grant of Vasiliki Stratigaki and research project no. FWO-3G029114), have been funded by the Research Foundation Flanders, Belgium (FWO).

REFERENCES

[1] B. Devolder, P. Rauwoens, P. Troch, Numerical simulation of a single Floating Point Absorber Wave Energy Converter using OpenFOAM®, in: 2nd Int. Conf. Renew. Energies Offshore, Lisbon, Portugal, 2016: pp. 197–205.

[2] OpenFOAM, OpenFOAM-3.0.1. (2015). http://www.openfoam.org/.

[3] J. Davidson, M. Cathelain, L. Guillemet, T. Le Huec, J. Ringwood, Implementation of an OpenFOAM Numerical Wave Tank for Wave Energy Experiments, in: Proc. 11th Eur. Wave Tidal Energy Conf., European Wave and Tidal Energy Conference, 2015.

[4] H.A. Wolgamot, C.J. Fitzgerald, Nonlinear hydrodynamic and real fluid effects on wave energy converters, Proc. Inst. Mech. Eng. Part A J. Power Energy. (2015). doi:10.1177/0957650915570351.

[5] J. Davidson, S. Giorgi, J. V. Ringwood, Linear parametric hydrodynamic models for ocean wave energy converters identified from numerical wave tank experiments, Ocean Eng. 103 (2015) 31–39. doi:10.1016/j.oceaneng.2015.04.056.

[6] P. Stansby, H. Gu, E.C. Moreno, T. Stallard, Drag minimisation for high capture width with three float wave energy converter M4, in: 11th Eur. Wave Tidal Energy Conf. (EWTEC 2015), Nantes, France, 2015.

[7] H.A. Wolgamot, P.H. Taylor, R. Eatock Taylor, The interaction factor and directionality in wave energy arrays, Ocean Eng. 47 (2012) 65–73. doi:10.1016/j.oceaneng.2012.03.017.

[8] A. Babarit, On the park effect in arrays of oscillating wave energy converters, Renew. Energy. 58 (2013) 68–78. doi:10.1016/j.renene.2013.03.008.

[9] J.C. McNatt, V. Venugopal, D. Forehand, A novel method for deriving the diffraction transfer matrix and its application to multi-body interactions in water waves, Ocean Eng. 94 (2015) 173–185. doi:10.1016/j.oceaneng.2014.11.029.

[10] E.B. Agamloh, A.K. Wallace, A. von Jouanne, Application of fluid-structure interaction simulation of an ocean wave energy extraction device, Renew. Energy. 33 (2008) 748–757. doi:10.1016/j.renene.2007.04.010.

[11] P.D. Mccallum, Numerical methods for modelling the viscous effects on the interactions between multiple wave energy converters, PhD manuscript, The University of Edinburgh, 2017.

[12] V. Stratigaki, P. Troch, T. Stallard, D. Forehand, J.P. Kofoed, M. Folley, M. Benoit, A. Babarit, J. Kirkegaard, Wave basin experiments with large wave energy converter arrays to study interactions between the converters and effects on other users in the sea and the coastal area, Energies. 7 (2014) 701–734. doi:10.3390/en7020701.

[13] C.W. Hirt, B.D. Nichols, Volume of Fluid (VoF) Method for the Dynamics of Free Boundaries, J. Comput. Phys. 39 (1981) 201–225. doi:10.1016/0021-9991(81)90145-5.

[14] B. Devolder, P. Rauwoens, P. Troch, Application of a buoyancy-modified k-ω SST turbulence model to simulate wave run-up around a monopile subjected to regular waves using OpenFOAM®, under review for Coast. Eng. (2017).

[15] B. van Leer, Towards the ultimate conservative difference scheme. II. Monotonicity and conservation combined in a second-order scheme, J. Comput. Phys. 14 (1974) 361–370. doi:10.1016/0021-9991(74)90019-9.

[16] P. Higuera, J.L. Lara, I.J. Losada, Realistic wave generation and active wave absorption for Navier-Stokes models. Application to OpenFOAM., Coast. Eng. 71 (2013) 102–118. doi:10.1016/j.coastaleng.2012.07.002.

[17] P. Higuera, J.L. Lara, I.J. Losada, Simulating coastal engineering processes with OpenFOAM., Coast. Eng. 71 (2013) 119–134. doi:10.1016/j.coastaleng.2012.06.002.

[18] B. Devolder, P. Schmitt, P. Rauwoens, B. Elsaesser, P. Troch, A Review of the Implicit Motion Solver Algorithm in OpenFOAM® to Simulate a Heaving Buoy, in: 18th Numer. Towing Tank Symp., Cortona, Italy, 2015.